

Supporting Information for

**Accelerating Electrochemical Hydrogen Evolution Kinetic in  
Alkaline Media Using LaNi<sub>5</sub> as a hydrogen reservoir**

Hang Shi,<sup>a</sup> Guoliang Liu,<sup>\*a</sup> and Xiaohong Hu<sup>\*a</sup>

*<sup>a</sup>Hubei Key Lab of Electrochemical Power Source, College of Chemistry and  
Molecular Sciences, Wuhan University, Wuhan, Hubei, 430072, China*

\*Corresponding author email: liugl@whu.edu.cn; xhhu88@whu.edu.cn;

## **Experimental Part:**

### **1. Chemicals and Reagents**

LaNi<sub>5</sub> (99.9 %) was purchased from Alfa Aesar. Cu powders (99.9%), Ag powders (99.9%) and oleylamine (AR) were purchased from Macklin. Potassium hydroxide (KOH, GR), Ni(NO<sub>3</sub>)<sub>2</sub>·6H<sub>2</sub>O (AR), NaH<sub>2</sub>PO<sub>2</sub>·H<sub>2</sub>O (AR), Cyclohexane (AR) and anhydrous ethanol (AR) were bought from Sinopharm Chemical Reagent. Deionized water (18.2 Mohm, Ultrapure system).

### **2. Synthesis of $\alpha$ -Ni(OH)<sub>2</sub>**

The synthesis procedure was according to the previous report.<sup>[1]</sup> In a typical method, 2 mmol (582 mg) of Ni(NO<sub>3</sub>)<sub>2</sub>·6H<sub>2</sub>O was put into 40 mL of ethanol with magnetic stirring. Then, 4 mL of oleylamine and 20 mL ethanol were added, and stirring for 30 min to form a homogenous solution. The formed clear solution was totally transferred into a 100 mL Teflon-lined autoclave, the autoclave was sealed and maintained at 180 °C for 15 h and then naturally cooled to room temperature. The obtained green precipitate was collected and washed with cyclohexane, ethanol and deionized water, and then dried under vacuum at 60 °C.

### **3. Synthesis of Ni<sub>2</sub>P**

To obtain Ni<sub>2</sub>P catalyst, 58.4 mg  $\alpha$ -Ni(OH)<sub>2</sub> and 800 mg NaH<sub>2</sub>PO<sub>2</sub>·H<sub>2</sub>O were put at two separate positions in a quartz boat, and NaH<sub>2</sub>PO<sub>2</sub>·H<sub>2</sub>O locates at the upstream side of furnace. Subsequently, the furnace was heated to 300 °C with a ramp rate of 3 °C min<sup>-1</sup> for 2 hours, the furnace was under Ar atmosphere with a flow rate of 60 mL min<sup>-1</sup>. After naturally cooled to room temperature, the prepared Ni<sub>2</sub>P sample was washed with deionized water and ethanol, and then dried under vacuum at 60 °C.

### **4. Construction of LaNi<sub>5</sub>-Ni<sub>2</sub>P, LaNi<sub>5</sub>-Ag and LaNi<sub>5</sub>-Cu complex catalysts**

In a typical procedure, the complex catalysts were prepared by a powder mix method. The two components were thoroughly mixed with a mortar and pestle. The LaNi<sub>5</sub> and Ni<sub>2</sub>P powder mixing configuration with a mass ratio of 1:1, 1:2 and 2:1 was prepared. The LaNi<sub>5</sub>-Ag and LaNi<sub>5</sub>-Cu with a mass ration of 1:1 was prepared to evaluate HER performance.

### **Structural and electrochemical characterization**

The X-ray diffraction (XRD) patterns were measured on a Rigaku Miniflex600

diffractometer with Cu  $K_{\alpha}$  radiation, All the samples were scanned from 10-80° with a scanning rate of 8°/min. The morphologies analysis was characterized by scanning electronics microscope (SEM, Zeiss Merlin Compact).

Electrochemical tests were performed at room temperature using a rotating disk working electrode with 5 mm glassy carbon (GC, 0.1962 cm<sup>2</sup>) connected to electrochemical workstation (CHI 660e). Hg/HgO (1 M KOH) and graphite rod were used as reference electrode and counter electrodes, respectively. The potential was calibrated to reversible hydrogen electrode (RHE) in 1 M KOH ( $E_{\text{RHE}}=E_{(\text{Hg}/\text{HgO})} + 0.924\text{V}$ ).

5 mg of catalyst powder was dispersed in 800  $\mu\text{L}$  of 1:1 v/v water/isopropyl alcohol mixed solvent with 20  $\mu\text{L}$  of 5 wt% Nafion solution. The mixture was then ultrasonicated for 30 min to form a homogeneous ink. Subsequently, 10  $\mu\text{L}$  of ink was transferred onto the 5 mm GC electrode disk, leading to a catalyst loading of 0.318 mg cm<sup>-2</sup>. The as-prepared catalyst film was dried at room temperature, 3  $\mu\text{L}$  of 0.5 wt% Nafion solution was then drop-casted onto the catalyst film to fix the catalyst.

The polarization curves were obtained by liner sweep voltammetry (LSV) method with iR drop correction at room temperature and 1200 rpm with a rotating disk electrode system, the sweep rate is 5 mV s<sup>-1</sup>. The electrochemical impedance tests were performed at different HER overpotential in the frequency range of 100 kHz-0.1 kHz with an amplitude of 5 mV. Chronoamperometry measure ( $j-t$ ) was carried out in 1 M KOH to evaluate the stability of LaNi<sub>5</sub>-Ni<sub>2</sub>P complex catalyst with 1 mg cm<sup>-2</sup> loaded on carbon paper.

The double layer capacitance ( $C_{\text{dl}}$ ) was taken to estimate the electrochemical activity surface area (ECSA) of a series of catalysts with a classic CV method at different scan rates (10, 30, 50, 70, 90 mV s<sup>-1</sup>) over a narrow range ( $\pm 50$  mV) centered around the open circuit potential (OCP).<sup>[2]</sup>

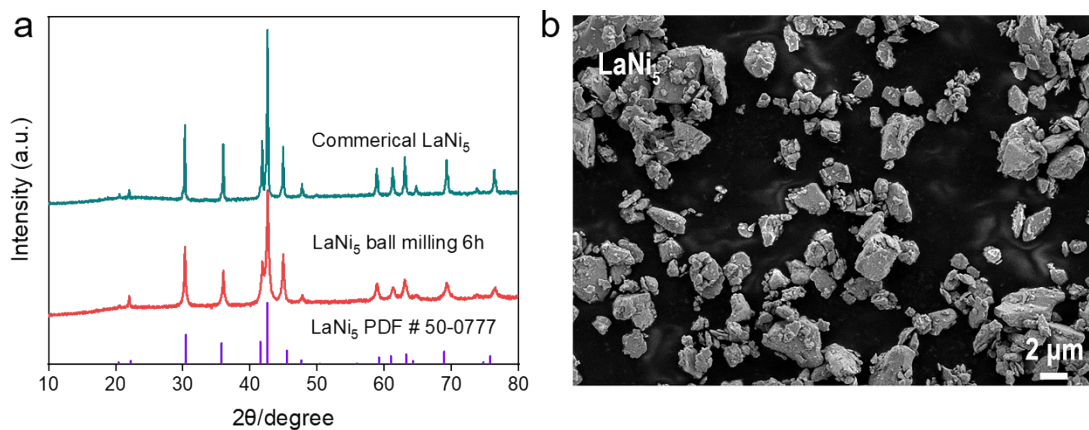


**Fig. S1** (a) XRD patterns of commercial  $\text{LaNi}_5$  and  $\text{LaNi}_5$  with 6 h ball milling, (b) SEM image of  $\text{LaNi}_5$  after 6 h ball milling.

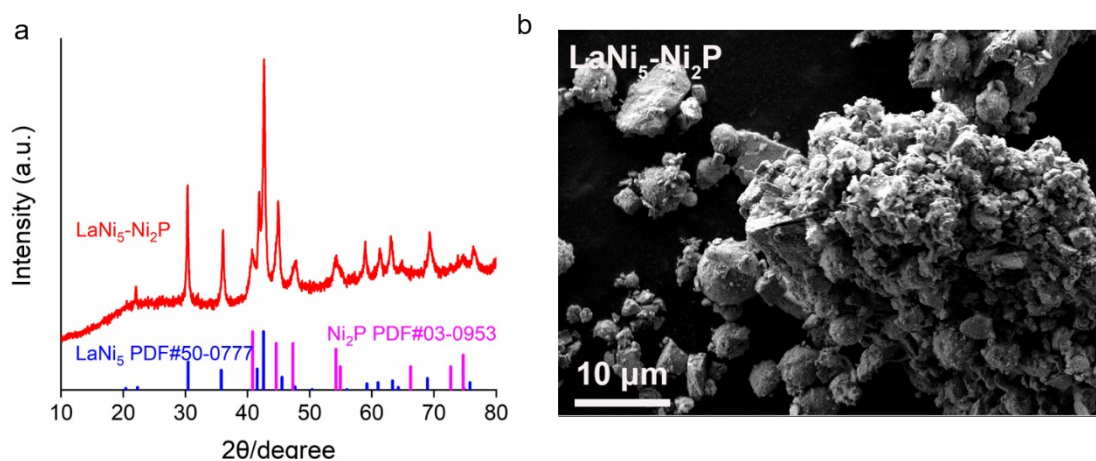


**Fig. S2** (a) XRD patterns of obtained  $\text{LaNi}_5\text{-Ni}_2\text{P}$ , (b) SEM image of  $\text{LaNi}_5\text{-Ni}_2\text{P}$  catalyst.

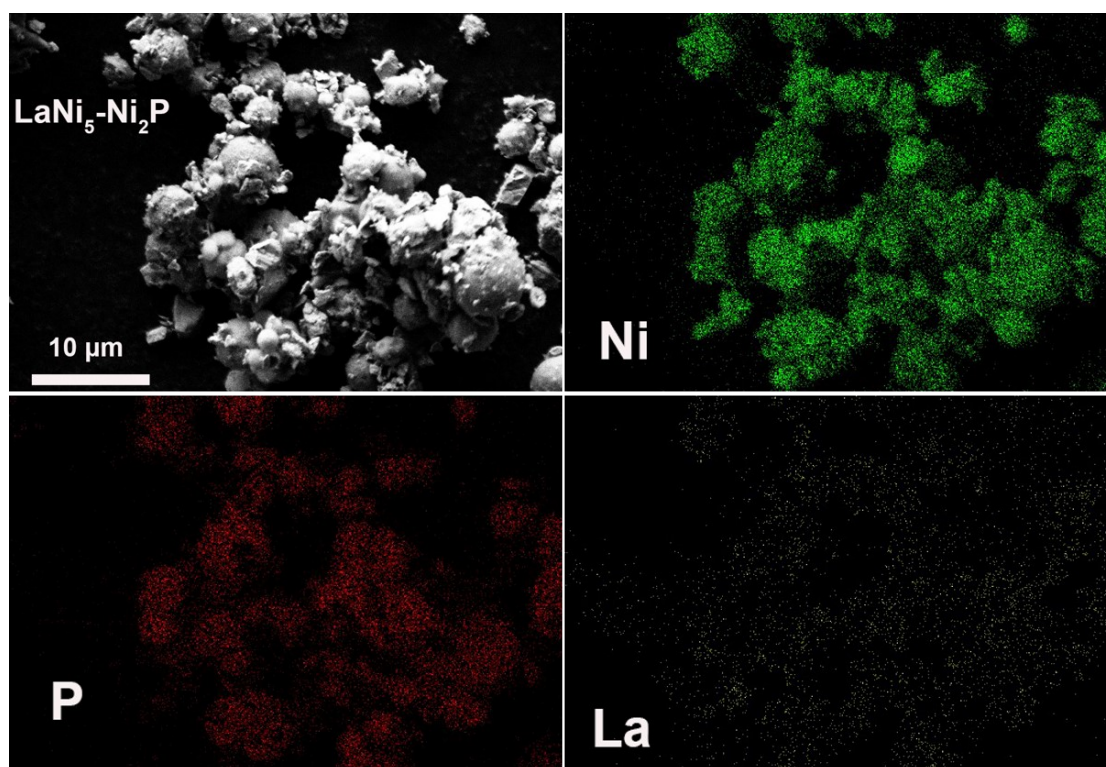


**Fig. S3** EDS mapping image of  $\text{LaNi}_5\text{-Ni}_2\text{P}$  complex

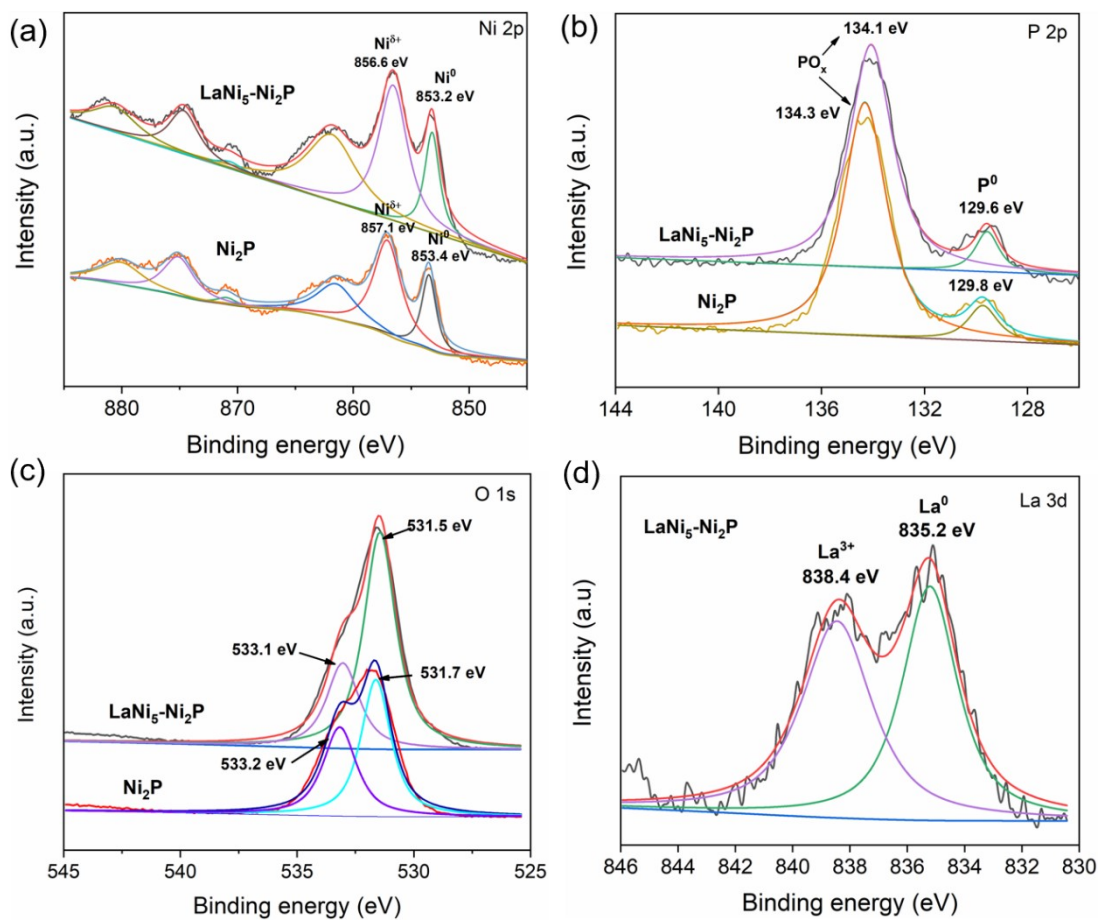


**Fig. S4** (a) Ni 2p and (b) P 2p (c) O 1s XPS spectra of LaNi<sub>5</sub>-Ni<sub>2</sub>P and Ni<sub>2</sub>P, (d) La 3d XPS spectra of LaNi<sub>5</sub>-Ni<sub>2</sub>P

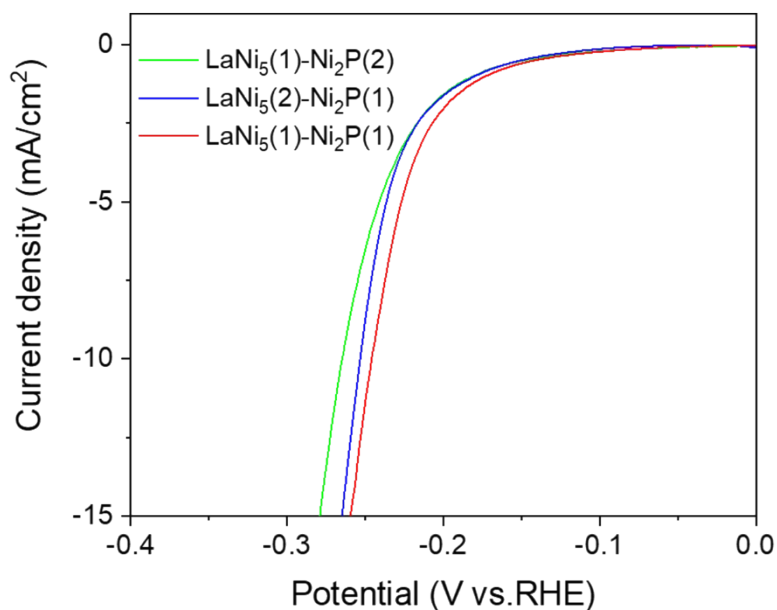


**Fig. S5** LSV curves of  $\text{LaNi}_5\text{-Ni}_2\text{P}$  complex catalyst mixed with different mass ratio,  $\text{LaNi}_5(1)\text{-Ni}_2\text{P}(1)$  presents the two parts mixed with a mass ratio of 1:1.

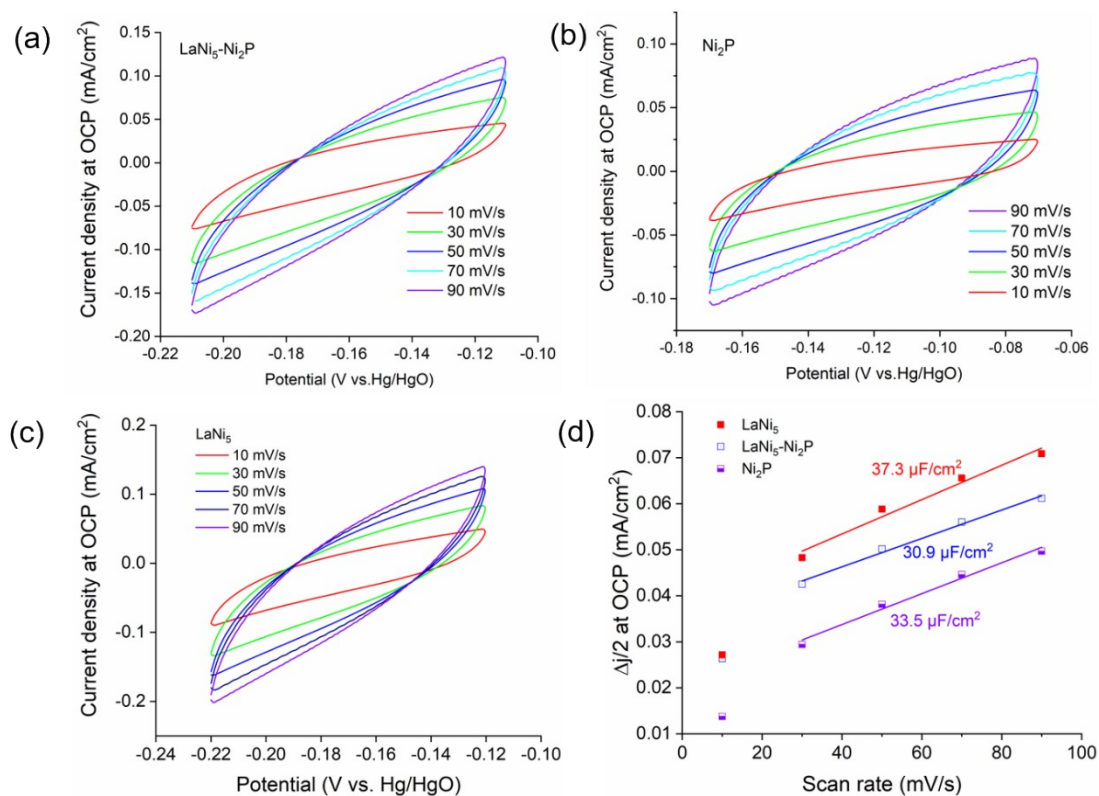


**Fig. S6** CV curves recorded at  $\text{OCP} \pm 50 \text{ mV}$  with different scan rates of (a)  $\text{LaNi}_5\text{-Ni}_2\text{P}$ , (b)  $\text{Ni}_2\text{P}$ , (c)  $\text{LaNi}_5$ . (d) Scan rate dependence of the current densities of  $\text{LaNi}_5\text{-Ni}_2\text{P}$ ,  $\text{Ni}_2\text{P}$ , and  $\text{LaNi}_5$  at OCP.



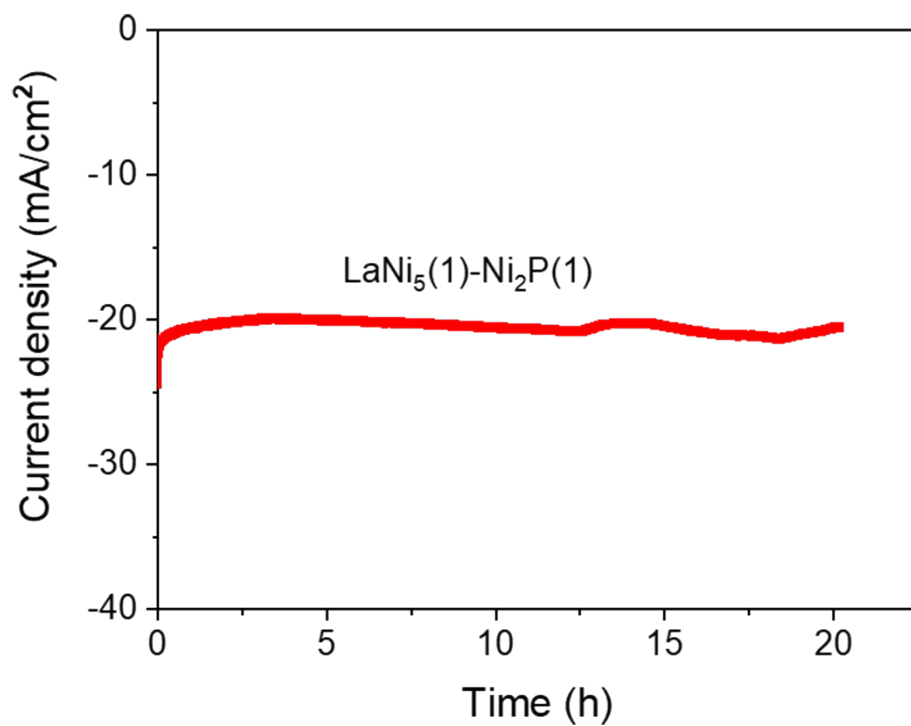


**Fig. S7** Chronoamperometry data ( $j-t$ ) recorded on LaNi<sub>5</sub>-Ni<sub>2</sub>P complex catalyst at a constant overpotential of 270 mV measured in 1 M KOH.

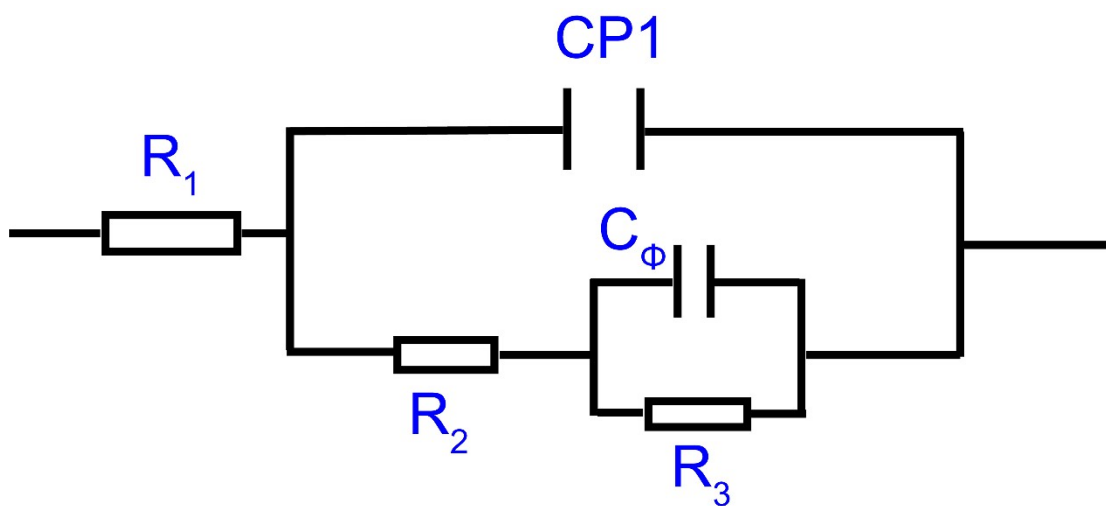


**Fig. S8** The equivalent circuit model for Nyquist plots.



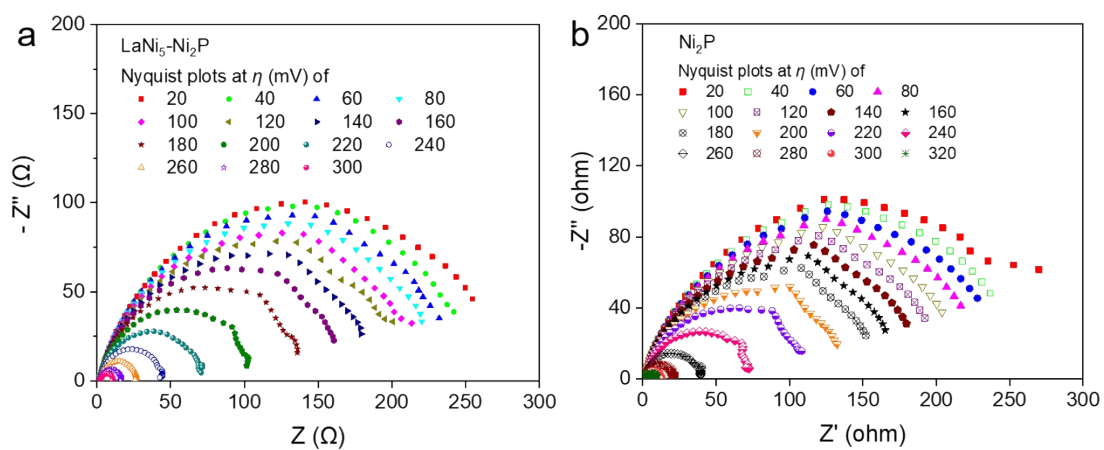


**Fig. S9** Nyquist plots for (a) LaNi<sub>5</sub>-Ni<sub>2</sub>P and (b) Ni<sub>2</sub>P catalyst in 1 M KOH at various HER overpotential ( $\eta$ )

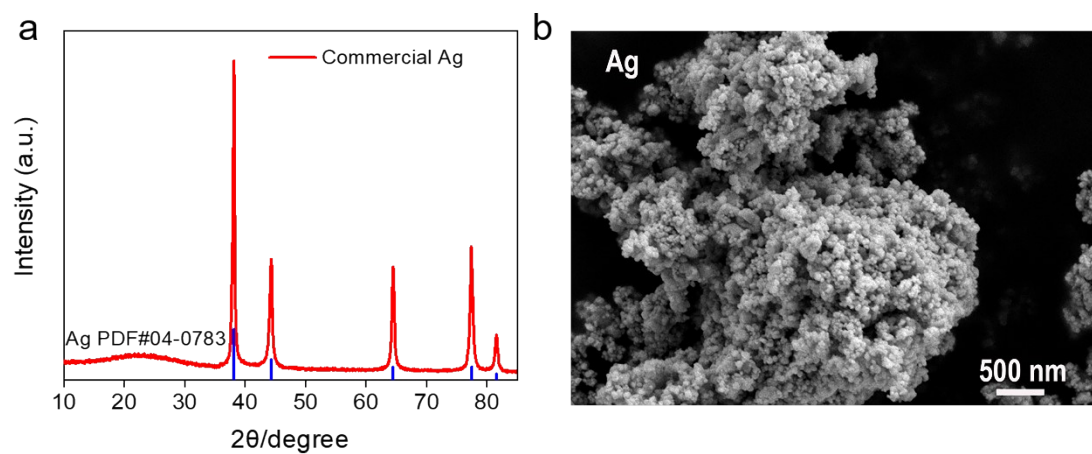


**Fig. S10** (a) XRD pattern (b) SEM image of commercial Ag powder.

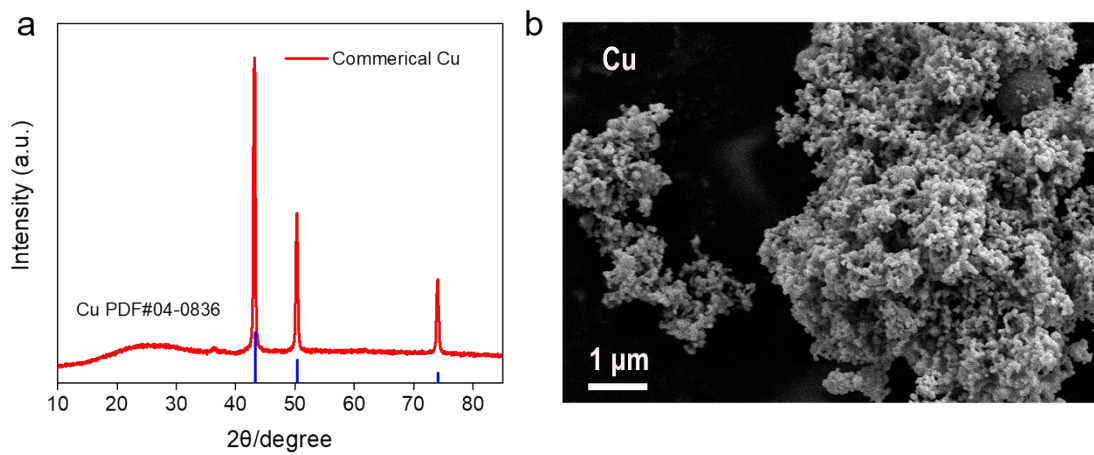


**Fig. S11** (a) XRD pattern (b) SEM image of commercial Cu powder.

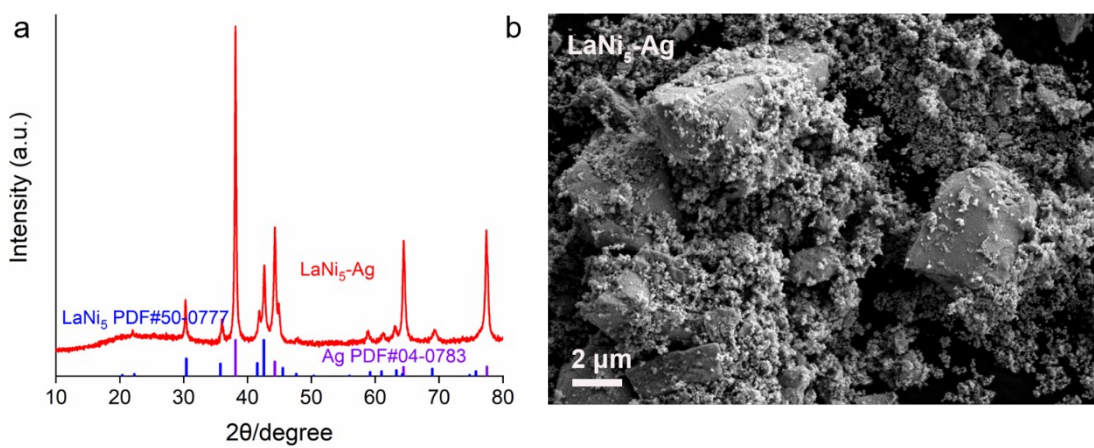


**Fig. S12** (a) XRD pattern and (b) SEM image of LaNi<sub>5</sub>-Ag complex.

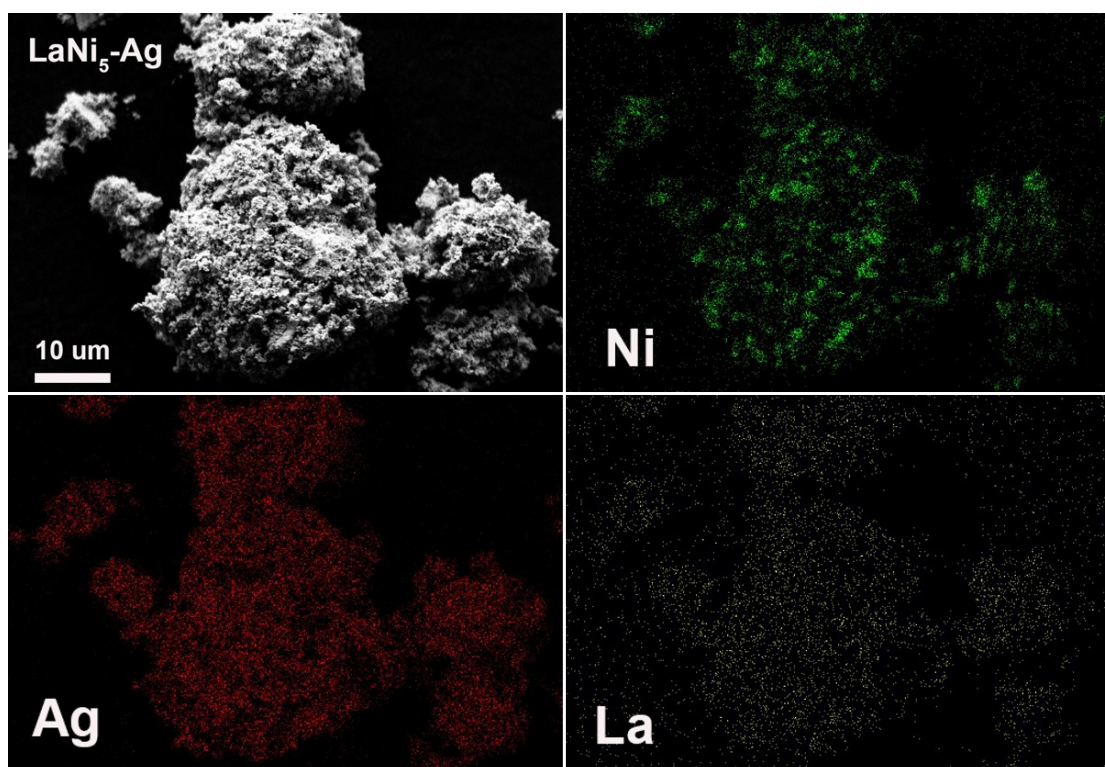


**Fig. S13** EDS mapping image of LaNi<sub>5</sub>-Ag complex

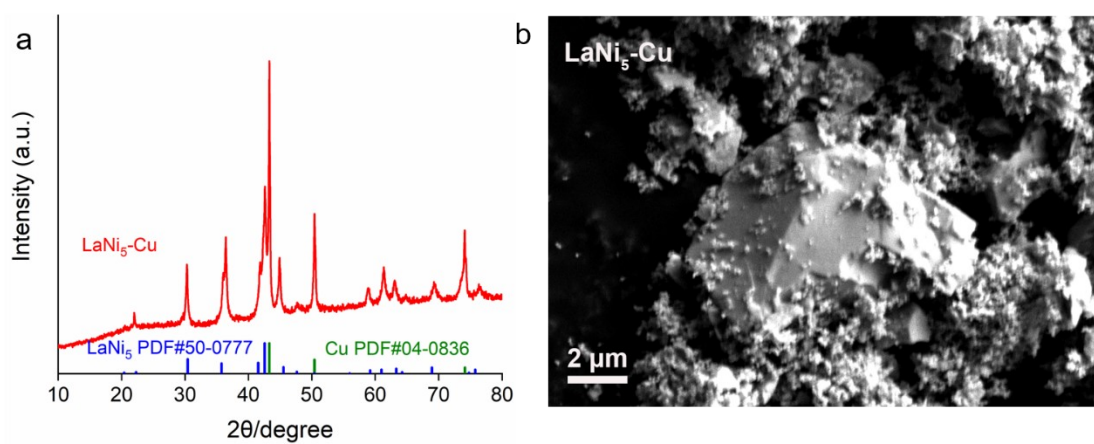


**Fig. S14** (a) XRD pattern and (b) SEM image of LaNi<sub>5</sub>-Ag complex.



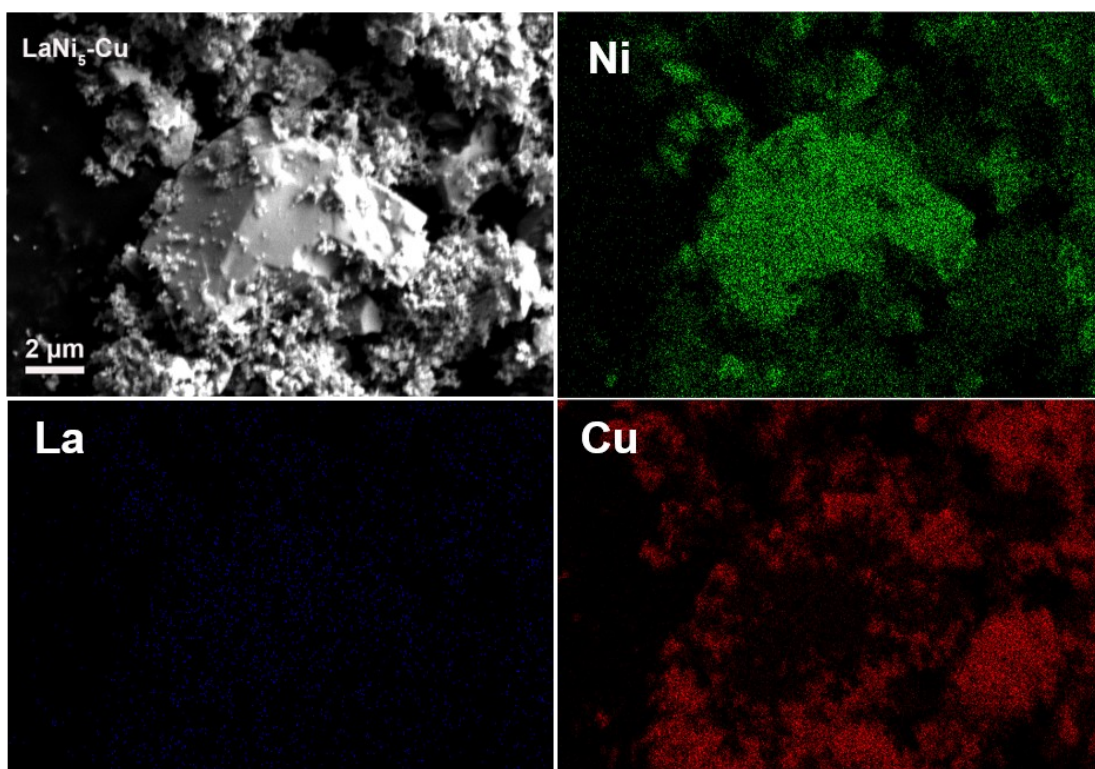


**Fig. S15** EDS mapping image of LaNi<sub>5</sub>-Cu complex

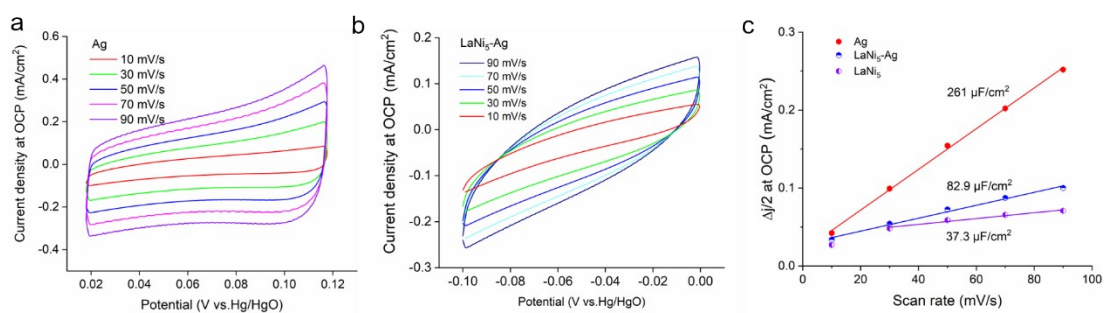


**Fig. S16** CV curves recorded at OCP ± 50 mV with different scan rates of (a) Ag, (b) LaNi<sub>5</sub>-Ag. (c) Scan rate dependence of the current densities of LaNi<sub>5</sub>-Ag, Ag, and LaNi<sub>5</sub> at OCP.

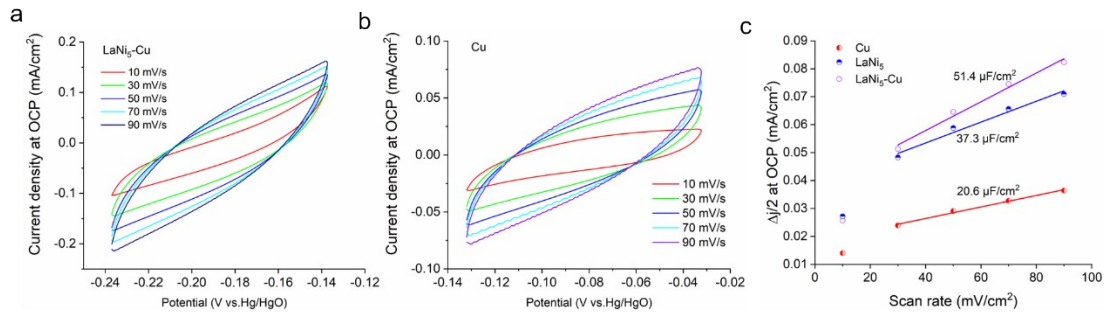


**Fig. S17** CV curves recorded at OCP  $\pm$  50 mV with different scan rates of (a) LaNi<sub>5</sub>-Cu, (b) Cu. (c) Scan rate dependence of the current densities of LaNi<sub>5</sub>-Cu, Cu, and LaNi<sub>5</sub> at OCP.

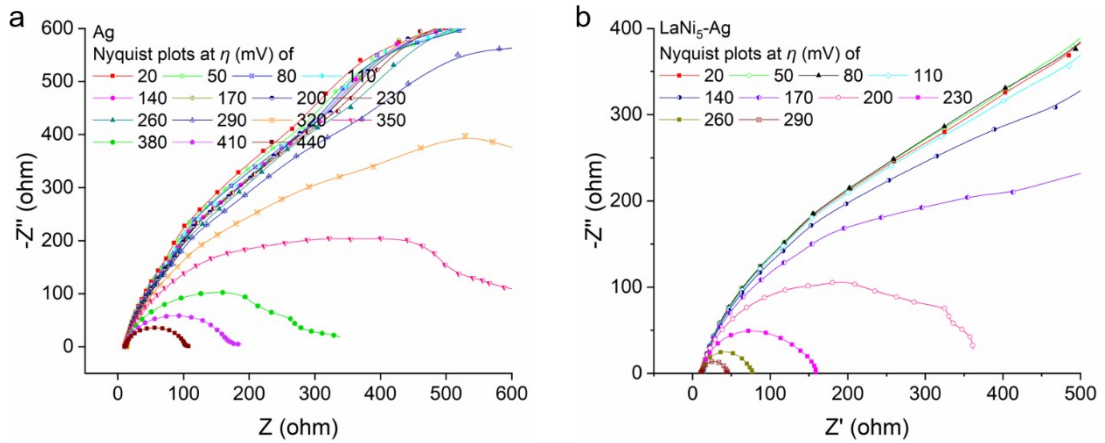


**Fig. S18** Nyquist plots for (a) Ag and (b) LaNi<sub>5</sub>-Ag catalyst in 1 M KOH at various HER overpotential ( $\eta$ )

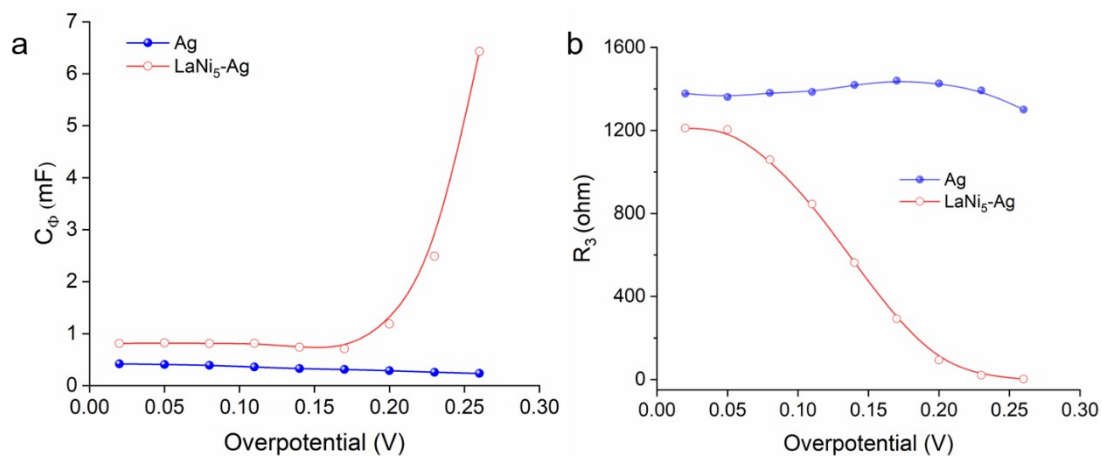


**Fig. S19** (a) Plots of hydrogen adsorption pseudo-capacitance ( $C_{\phi}$ ) vs different overpotential for LaNi<sub>5</sub>-Ag and Ag (b) Plots of hydrogen adsorption resistance ( $R_3$ ) vs different overpotential for LaNi<sub>5</sub>-Ag and Ag.

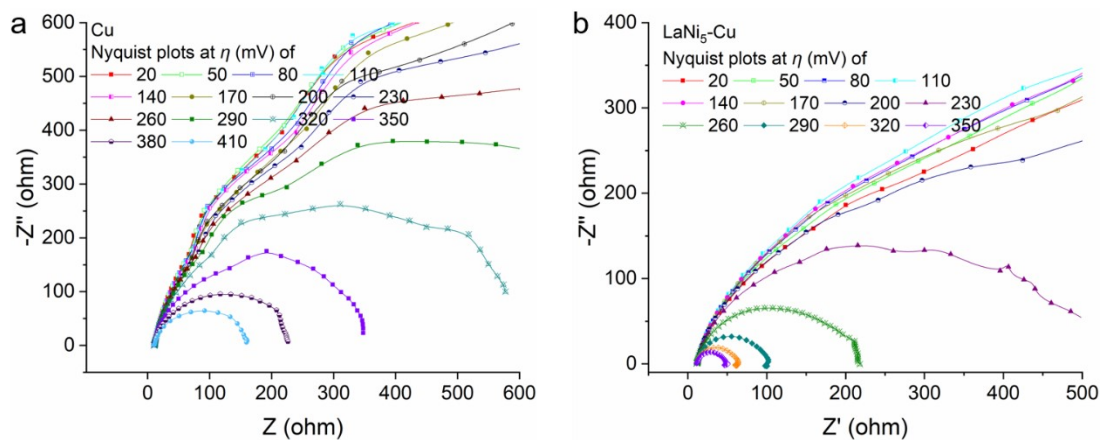


**Fig. S20** Nyquist plots for (a) Cu and (b) LaNi<sub>5</sub>-Cu catalyst in 1 M KOH at various HER overpotential ( $\eta$ )

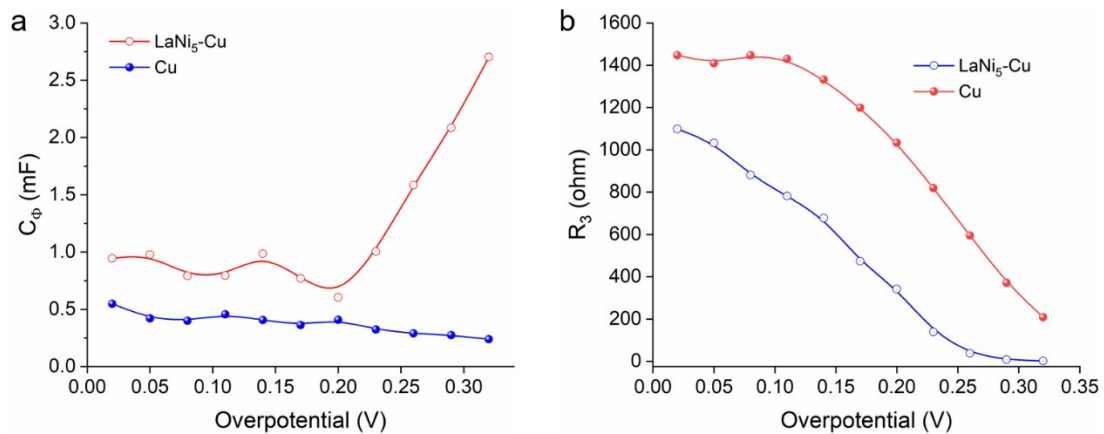


**Fig. S21** (a) Plots of hydrogen adsorption pseudo-capacitance ( $C_p$ ) vs different overpotential for LaNi<sub>5</sub>-Cu and Cu (b) Plots of hydrogen adsorption resistance ( $R_3$ ) vs different overpotential for LaNi<sub>5</sub>-Cu and Cu.



**Table S1.** Comparison of HER performance in 1 M KOH with some advanced catalysts

Catalysts	Substrate	Loading (mg/cm <sup>2</sup> )	$\eta_{10}$ (mV)	Tafel slope (mV/dec)	Reference
NiMo <sub>3</sub> S <sub>4</sub>	Glassy carbon electrode (GCE)	0.3	257	98	<i>Angew. Chem. Int. Ed.</i> <b>2016</b> , 55, 1-6
Ni <sub>2</sub> P	Ni foam	1.8	221	N/A	<i>Energy Environ. Sci.</i> <b>2015</b> , 8, 2347-2351
NiN <sub>4</sub> -Cl SAs/N-C	GCE	N/A	243	89.2	<i>J. Mater. Chem. A</i> , <b>2022</b> , 10, 6007-6015
Hierarchical Ni <sub>2</sub> P	GCE	0.283	298	108	<i>Chem. Mater.</i> <b>2017</b> , 29, 8539–8547
Ni-S-B	Nickel mesh	N/A	240	140	<i>Applied Surface Science</i> , <b>2019</b> , 480, 689-696
Quasi-Amorphous Metallic Nickel	GCE	0.26	240	140	<i>Adv. Sci.</i> <b>2018</b> , 5, 180146
Ni/NiO	GCE	0.25	226	135	<i>Electrochimica Acta</i> , <b>2020</b> , 361, 137040
LaNi <sub>5</sub> -Ni <sub>2</sub> P	GCE	0.31	245	67.1	
LaNi <sub>5</sub> -Ag	GCE	0.31	278	52.3	This work
LaNi <sub>5</sub> -Cu	GCE	0.31	290	86.9	

## References:

- [1]. M. Gao, W. Sheng, Z. Zhuang, Q. Fang, S. Gu, J. Jiang and Y. Yan, Efficient Water Oxidation Using Nanostructured  $\alpha$ -Nickel-Hydroxide as an Electrocatalyst, *J. Am. Chem. Soc.*, 2014, **136**, 7077-7084.
- [2]. Y. Yoon, B. Yan and Y. Surendranath, Suppressing Ion Transfer Enables Versatile Measurements of Electrochemical Surface Area for Intrinsic Activity Comparisons, *J. Am. Chem. Soc.*, 2018, **140**, 2397-2400.